Peter Knödel

ELSEVIER

Thin-Walled Structures 23 (1995) 283–293

0263-8231/95/$9.50

0263-8231(95)00017-8

On the Modelling of Different Types of Imperfections in Silo Shells

Peter Knoedel, Thomas Ummenhofer & Ulrich Schulz

Versuchsanstalt für Stahl, Holz und Steine, University of Karlsruhe, Karlsruhe, Germany

ABSTRACT

The assessment of imperfections is most important for determining the load-bearing capacity of a thin-walled shell structure. Different ways of modelling imperfections are discussed in this paper and steel silo shells are used as an application. Buckling tests were performed on different types of model shell — standard quality and high quality with reduced heat input during welding. For the numerical studies two different approaches were used as well: an axisymmetric approach with substitute geometric imperfections and an FEM approach, where the nodal coordinates were derived from surveying the specimen. It was found that there is considerable gain in the buckling strength due to the presence of the granular solid. The larger the initial imperfections in the shell the greater the gain in strength compared to the empty cylinder. The modelling of the uneveness of the edges with uneven dead loading is also discussed.

1 INTRODUCTION

It is commonly agreed that it is the presence of imperfections which is the reason for a wide scatter band of real shell ultimate loads; these range from the *classical buckling load* (see eqn (1)) to less than 10% of that load, depending upon the geometrical and physical parameters of the individual shell. If suitable input data are available, the structural stability can be estimated by use of numerical tools. Imperfection data banks are available for aircraft structures. For civil and mechanical engineering structures, very few imperfection measurements are known.

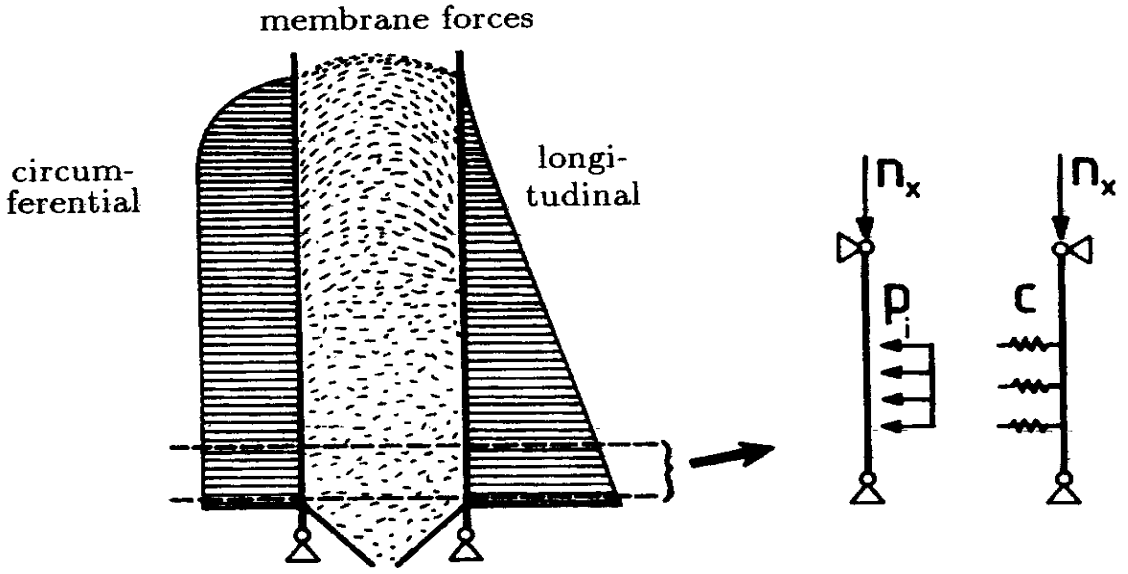

Fig. 1. Deterministic, axisymmetric loads in silos.

With silo shells an additional problem arises because the interaction of the shell and the bulk solid is not very well known. In modelling, we use a simple axisymmetric approach neglecting all irregularities in flow patterns as well as time effects (see Fig. 1).

We model the presence of the bulk solid by an internal pressure and a linear radial stiffness, similar to a Winkler foundation. Since the shell wall might lose contact with the bulk solid's core while moving outward, and the bulk solid might become plastic when the shell wall moves inward, we introduced nonlinearities into the pressure–displacement law.

In a first simple model, we use axisymmetric imperfections and evenly distributed axial compression. The imperfections of the model are meant to be substitute geometric imperfections, which account for all geometrical deviations, inhomogenities of the shell material, misalignments in loading, etc. The imperfections are calibrated in a way that should ensure a lower bound of the structural behaviour of the shell. In this way, the results of the structural analysis can be directly used for structural design.

In a second, more sophisticated, approach we surveyed specimens using a grid 20 mm × 20 mm, so that 9400 nodal coordinates were available for the FEM model. In addition, we introduced uneven edge loading by using strain-gauge readings from the experimental tests.

2 EXPERIMENTS

In our experiments, we used cylindrical model shells with the following nominal properties: $R = 625$ mm, $L = 1000$ mm, $T = 0{\cdot}63$–$1{\cdot}0$ mm, giving

$R/T = 650$–1000. The models were formed from sheet steel with yield limits $f_y = 180$–$360\,\mathrm{N/mm^2}$, giving a normalized slenderness $\bar{\lambda} = \sqrt{f_y/\sigma_{cl}} = 0{\cdot}8$–$1{\cdot}2$, where

$$\sigma_{cl} = \frac{E}{\sqrt{3(1-\nu^2)}}\frac{T}{R} \approx 0{\cdot}605\,E\frac{T}{R} \tag{1}$$

is known as the classical buckling load. Flanges of 60 mm width were attached to both ends of the cylinder.

Two different types of model shell were manufactured:

- Standard quality specimens. The longitudinal overlap was tack-welded, L-flanges $30 \times 60 \times 5$ mm were gas-shielded, metal-arc welded to the edges of the shell. The models were machined at both ends. Further details are given in Refs 1 and 2.
  The planned-to-be 'realistic' geometrical imperfections turned out to be longitudinally orientated folds rather than circumferentially orientated bulges, as would be expected for real welded structures. A typical example is shown in Fig. 2. The shortcoming of these imperfection patterns in our models was pointed out by Rotter and Zhang previously;[3] the relevance with respect to the assessing of real structures will be discussed later.
- High quality specimens[4] with 'controlled' imperfections. In a second set of experiments, we planned to manufacture specimens for a direct comparison with numerical calculations rather than to mirror 'realistic' imperfections. Imperfections that are difficult to determine in distribution and magnitude, such as residual stresses, were decided to be reduced to the lowest possible amount. Imperfections that cannot be reduced, such as geometrical deviations, were surveyed very

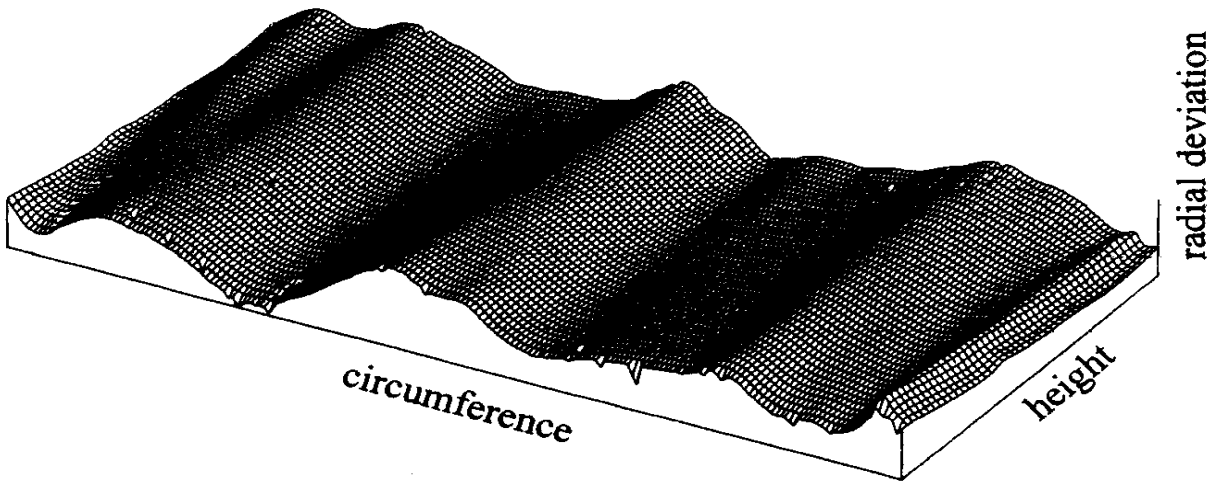

Fig. 2. Surveyed shape of shell A.

carefully, so that the real shape of the specimen could be introduced into the numerical calculations. The longitudinal seam was laser butt-welded and annular rings 10 × 60 mm were TIG pulse welded to the outside of the shell edges, in order to input minimum heat into the shell material. The models for pure axial compression had a pair of symmetrical rings glued to each end by means of epoxy resin. All models were machined at both ends. Further details are given in Ref. 4.

Both types of model shell were subjected to the following:

- Pure axial compression.
- Axial compression and simultaneous internal pressure, where the internal pressure was introduced by a water fill. The buckling coefficient given in Fig. 3 describes the *top edge* of the specimen.
- Sand fill, where the wall friction induces axial compression simultaneously with the normal wall pressure.
- Sand fill and additional axial compression, where the additional axial compression increases the membrane compression for a given sand height.

A selection of the buckling coefficients $\alpha = \sigma_u/\sigma_{cl}$ which were found in the experiments are plotted in Fig. 3. The different levels of results (solid and hollow markers) account for the different quality of edge preparation and welding described above.

The following conclusions can be drawn from the results in Fig. 3:

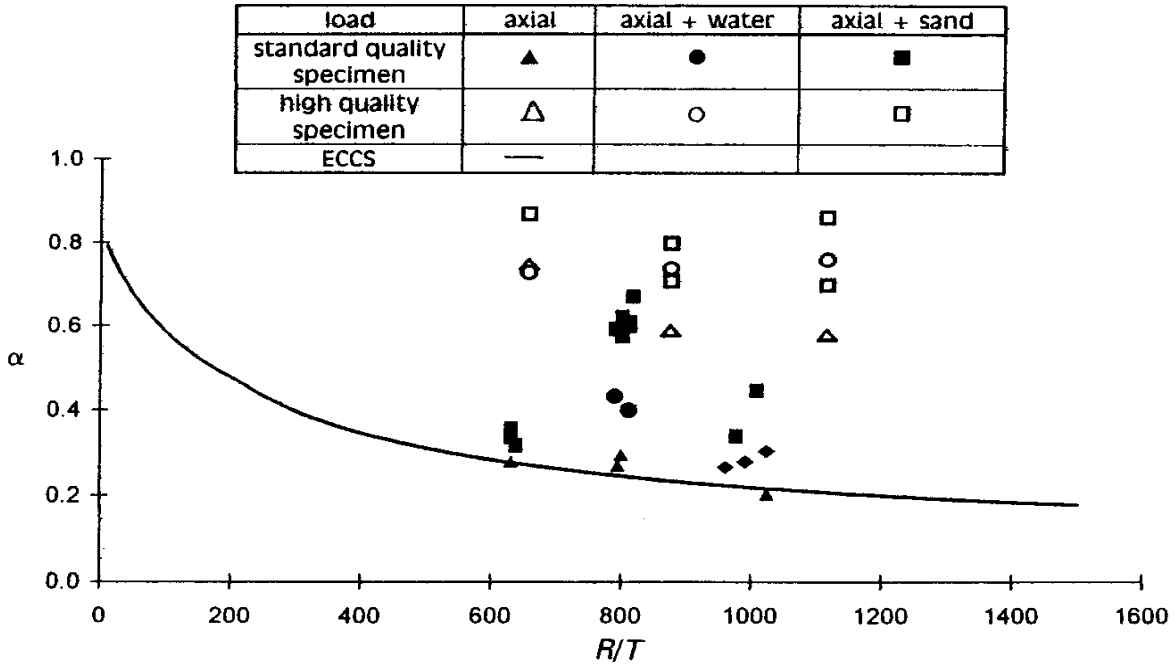

Fig. 3. Experimental results.

- sand can increase the buckling strength as much as 100% for a specimen with realistic imperfections;
- much of this gain results from the bulk solid's stiffness;
- no gain can be expected with plastic buckling.
  (In plastic buckling, bulges develop on the outside of the shell, where the bulk solid is not of much benefit.)

3 NONLINEAR LAW OF WALL PRESSURES

In the numerical calculations, the presence of the granular solid was modelled by a velocity-independent material law (simplified, according to Rombach[5]) which gives the wall pressures as shown in Fig. 4.

For academic reasons, the pressure versus displacement path has been split into a constant internal pressure and a nonlinear radial stiffness ('foundation') of the wall. The modulus of the stiffness depends upon the (vertical) compression of the granular material (compare Refs 3 and 6).

4 APPROACH I: AXISYMMETRIC SUBSTITUTE IMPERFECTIONS

The computer code of Wunderlich *et al.* has been used to model substitute axisymmetric imperfections and axisymmetric prebuckling states of the shell. The code has been described elsewhere.[7]

To obtain a shell of medium length, the dimensions of the shell were chosen as $R = 1000\,\text{mm}$, $T = 1\,\text{mm}$, $L = 500\,\text{mm}$. Young's modulus was

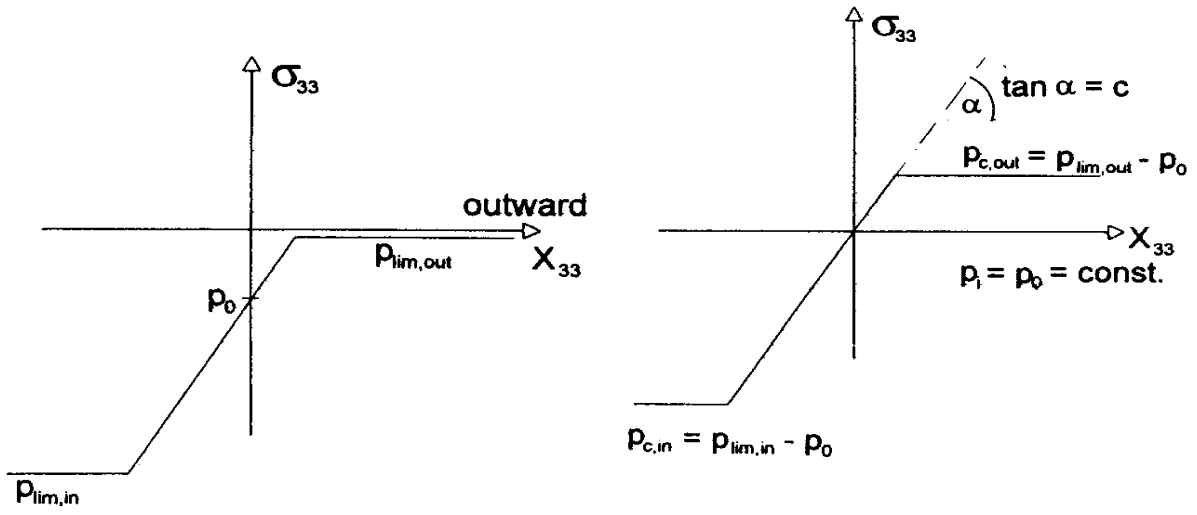

Fig. 4. Nonlinear law of wall pressures.

taken as $E = 2{\cdot}0 \times 10^5\,\mathrm{N/mm^2}$, Poisson's ratio $\nu = 0{\cdot}3$ and the yield limit $f_y = 240\,\mathrm{N/mm^2}$. For reasons of comparison, the boundary conditions were taken as simply supported at both edges.

Shell structures in civil and mechanical engineering are joined by welding single strakes. Due to weld shrinkage the governing initial imperfections are orientated in the circumferential direction. Axisymmetric imperfections have been found to be most deleterious to the stability of cylindrical shells both for pure axial compression and axial compression with simultaneous internal pressurization.[8]

Following the widely used concept of eigenmode-shaped geometric imperfections, the lowest bifurcation load which is coupled to an axisymmetric eigenmode was determined for the initially perfect cylinder. For pure axial compression, this shape was found to have nine halfwaves along the meridian. The membrane stress at the calculated ultimate load is $54\,\mathrm{N/mm^2}$ ($\alpha = \sigma_u^{imp}/\sigma_{cr}^{perf} = 0{\cdot}50$), first yield is detected at $43\,\mathrm{N/mm^2}$ ($\alpha = \sigma_u^{imp}/\sigma_{cr}^{perf} = 0{\cdot}40$) and bifurcation is found at $29\,\mathrm{N/mm^2}$ ($\alpha = \sigma_{cr}^{imp}/\sigma_{cr}^{perf} = 0{\cdot}27$). The corresponding eigenmode has $N = 17$ circumferential waves and two halfwaves along the meridian. These results are in good agreement with the findings of other researchers for $R/T = 1000$ (e.g. Teng and Rotter[9]).

For a stiffness of the bulk solid of $c = 0{\cdot}0063\,\mathrm{N/mm^3}$ and an internal pressure $p_i = 0{\cdot}012\,\mathrm{N/mm^2}$, bifurcation and first yield are found at $43\,\mathrm{N/mm^2}$; this is a strength gain of some 45% (see Section 5.3).

5 APPROACH II: SIMULATION OF MEASURED IMPERFECTIONS

5.1 General*

The ANSYS 4.4 and 5.0 codes were used to introduce the measured imperfections into an FEM analysis. The actual geometry was taken from a surveyed test specimen, following a grid of approximately $20\,\mathrm{mm} \times 20\,\mathrm{mm}$, which gives 9400 nodes per shell. Edge load distributions were taken from strain gauge measurements prior to failure of the specimen.

An isoparametric four-node non-flat shell element (STIFF43/SHELL43) was used. The element is based on continuum theory with one condensed dimension and is therefore independent of any specific shell theory.

*The results presented in this section are part of the PhD thesis of the second author.

Various boundary conditions were investigated; in the comparison with the experiments, fully clamped edges were used.

A nonlinear analysis was employed and instability points were detected by observing the main diagonal elements of the stiffness matrix. Critical points were determined with an accuracy of 1% of the failure load of the respective specimen by use of bisection.

5.2 Radial deviations

When the measured radial deviations were used for the nodal coordinates of the numerical model, failure was detected at $\alpha = \sigma_u/\sigma_{cl} = 0{\cdot}65$–$0{\cdot}83$ (see Table 1, shells A–C). This compares to the buckling coefficient of the perfect cylinder with clamped edges which can be assumed to be $\alpha = \sigma_u/\sigma_{cl} = 0{\cdot}925$ according to Yamaki.[10]

5.3 Imperfection depth

Figure 5 shows the influence of different imperfection depths for a given imperfection pattern (see Section 5.2). For $w_{0,max}/T \approx 1$, a knock-down factor of $\alpha \approx 0{\cdot}8$ was obtained for a cylinder under pure axial compression. The values obtained with the axisymmetrical approach presented above, as well as the results known from the literature (e.g. Teng and Rotter for $R/T = 1000$[9] and Haefner for $R/T = 500$[11]), are of the order of $\alpha \approx 0{\cdot}3$. This difference is due to two facts:

- Axisymmetric imperfection patterns have been used in Refs 9 and 11. These patterns are more deleterious to the buckling load than the

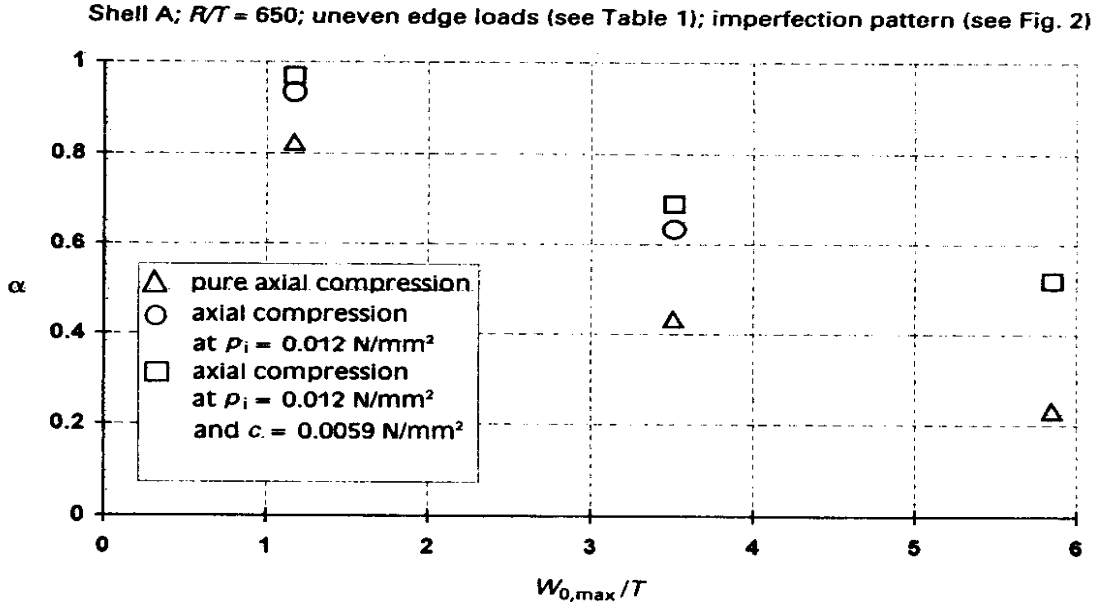

Fig. 5. Buckling coefficients vs max. imperfection depth.

imperfection pattern of the investigated specimen, which looks rather like longitudinal waves.

- Along the abscissa of Fig. 5 $w_{0,\max}/T$ is plotted, which is the maximum distance between the best-fit perfect cylinder and the actual surface of the specimen. Therefore, $w_{0,\max}/T = 1$ in Fig. 5 indicates a certain global deviation rather than a local imperfection of the same depth.

The beneficial effect of the stiffness of a bulk solid inside a silo is shown in Fig. 5 as well. According to the real dimensions of our test silo, and the quartz sand used, a stiffness $c = 0{\cdot}0059\,\mathrm{N/mm^3}$ of the granular material was chosen as a lower bound. Further discussion on different ways to determine an appropriate stiffness is given in Ref. 12.

In common design practice, an internal quasi-pneumatic pressure is taken into account, which is equivalent to the bulk solid's wall pressure at rest. The corresponding critical loads are plotted for comparison in Fig. 5, where an internal pressure of $p_i = 0{\cdot}012\,\mathrm{N/mm^2}$ was used. This pressure is expected (according to German Standard DIN 1055 part (6)) to be the pressure of the bulk solid at rest at the top edge of the specimen. This shows that the strength gain due to the bulk solid's stiffness is larger for deeper imperfections. For $w_{0,\max}/T = 1$, the gain is about 30% compared to the empty cylinder. With the axisymmetric approach in Section 4, a gain of 45% was found. This confirms the previous finding, since it was pointed out above that the effective imperfection depth is bigger in the axisymmetric approach.

5.4 Uneven edge loads

As a further step to improve the modelling, the uneven edge load distribution, which has been measured in the experiments (see Section 2), was introduced into the numerical model.

The load patterns for the top and bottom ends were taken from the strain gauge recordings (membrane components only), which were obtained in the last stable load step before failure of the specimen. These load patterns were linearly scaled up to failure load.

Table 1 shows a sample of results obtained for different R/T ratios and boundary conditions. Due to the uneven edge loads, $\alpha = \sigma_u/\sigma_{cl}$ could not be used to define the buckling coefficient in Table 1. Instead of defining $\alpha = \sigma_{u,\max}/\sigma_{cl}$ which could give misleading results in some cases, the ratio of the total compressive loads $\alpha = N_u/N_{cl}$ was used. This shows that the decrease due to the uneven edge loads ranges from -1% to -30%, being smaller for the small R/T ratios. It seems that the combination of a high edge load peak and a deep local imperfection along the same meridian

TABLE 1
Effect of Uneven Edge Loads: Numerical Results for $\alpha = N_u/N_{cl}$

Shell			*A*	*B*	*C*	*D*	*E*	*F*
Condition			empty	empty	empty	water	water	water
R/T			650	850	1100	650	850	1100
$w_{0,max}/T$			1·83	2·72	2·33	1·84	3·04	2·58
Boundary conditions			Clamped			Clamped		
$\alpha = N_u/N_{cl}$ (even)			0·76	0·65	0·83	0·94	0·96	1·00
$\alpha = N_u/N_{cl}$ (uneven)			0·75	0·62	0·59	0·85	0·90	0·77
(difference to even in %)			−1	−5	−29	−10	−6	−23
Uneveness of meridional membrane stresses (% of mean)	Top	Max	+18	+18	+19	+11	+12	+33
		Min	−8	−14	−15	−11	−22	−55
	Bottom	Max	+7	+12	+34	+17	+24	+30
		Min	−13	−16	−22	−13	−24	−46

triggers premature failure of the shell (compare shell C and shell F in Table 1).

6 CONCLUSIONS

The 'standard quality specimens' seemed to represent ordinary steel structures reasonably well ($\alpha \approx 0{\cdot}3$ for an empty cylinder under axial compression), although they appear to have quite a different imperfection pattern. For these specimens, an increase of the buckling stress of 100% due to the presence of the granular solid was found.

'High quality specimens' were manufactured with minimized heat input during welding. This gives a very low level of residual stresses, which allows one to compare the buckling loads obtained directly with the numerical calculations. As a result of the low residual stresses, buckling coefficients close to 0·6 for a shell $R/T = 1100$ under pure axial compression were obtained.

Steel shell structures of civil and mechanical engineering are usually made up of different strakes, which are joined by welding. The governing imperfection pattern, which is induced through weld shrinkage, consists of single circumferential bulges. Therefore, when designing a shell, it is justified to use a simple axisymmetric imperfect model for analysis.

The specimen used in the above tests and the models used in the FEM

analysis had longitudinal folds rather than circumferential bulges. For this reason the buckling coefficients turned out to be rather high, even if the maximum deviations from the best-fit cylinder ranged from 1·8 to 3·0 wall thicknesses.

Using uneven edge loading in a numerical analysis (as presented in Section 5.4) is only a rough estimate of the situation in an experimental test setup. The uneven stress distribution along the edges of the specimen results from the uneveness of the surfaces (machined ends of the specimen and loading plates) in contact. Thus, the development of the stresses is a matter of the deformation-controlled fitting of the adjacent surfaces. The stability of the structure depends upon these stiffness restraints at the boundaries. In modelling this situation by unevenly distributed loads, the stiffness restraints are changed into prescribed stress resultants. The stability of the structure depends then upon its own stiffness exclusively.

Correct results could be obtained by the use of gap elements only, but this requires an enormous amount of numerical effort due to the highly nonlinear behaviour. Since width and depth of the actual gaps cannot be measured in the experiment, it is very difficult to calibrate the gaps to a given stress distribution.

For the above reasons, it is obvious that modelling with dead loads is a necessity from the engineering point of view. Our studies and the comparison of numerical analyses and experiments (which have not been presented in this paper) indicate that the accuracy of this procedure is sufficient.

ACKNOWLEDGEMENT

This work has been funded by the German Research Foundation (DFG). This is gratefully acknowledged.

REFERENCES

1. Knoedel, P. & Schulz, U., Buckling of silo bins loaded by granular solids. In *Proc. Silos — Research and Experience, Conf. '88.* SFB 219. University of Karlsruhe, 10–11 October 1988, pp. 287–302.
2. Knoedel, P. & Schulz, U., Buckling of cylindrical bins — recent results. In *Proc. Silos — Research and Practice, Conf. '92.* SFB 219. University of Karlsruhe, 8–9 October 1992, pp. 75–82.
3. Rotter, J. M. & Zhang, Q., The strengthening effect of stored solids on the buckling of cylindrical steel silos. *Proc. 3rd. Int. Conf. on Bulk Materials, Storage, Handling and Transportation*, Newcastle 27–29 June 1989, Inst. of Engineers, Australia.

4. Knebel, K., Peil, U., Schulz, U., Schweizerhof, K. & Ummenhofer, T., Sonderforschungsbereich 219: Silobauwerke und ihre spezifischen Beanspruchungen. Arbeits- und Ergebnisbericht für die Jahre 1990–1992. University of Karlsruhe, April 1993, pp. 135–70.
5. Rombach, G., Schüttgutbeanspruchungen von Silozellen — Exzentrische Entleerung. PhD thesis, University of Karlsruhe, 1991.
6. Nielsen, J. & Kolymbas, D., Properties of granular media relevant for silo loads. In *Proc. Silos — Research and Experience, Conf. '88*. SFB 219. University of Karlsruhe, 10–11 October 1988, pp. 119–32.
7. Wunderlich, W., Cramer, H. & Obrecht, H., Application of ring elements in the nonlinear analysis of shells of revolution under nonaxisymmetric loading. *Comp. Meth. Appl. Mech. Engng*, **51** (1985) 259–75.
8. Hutchinson, J., Axial buckling of pressurized imperfect cylindrical shells. *AIAA J.*, **3** (1965) 1461–6.
9. Teng, J. G. & Rotter, J. M., Buckling of pressurized axisymmetrically imperfect cylinders under axial load. *J. Engng Mech.*, **118** (1992) 229–47.
10. Yamaki, N., *Elastic Stability of Circular Cylindrical Shells*. North-Holland Series in Applied Mathematics and Mechanics, North-Holland, Amsterdam, 1984.
11. Haefner, L., Einfluss einer Rundschweissnaht auf die Stabilität und Traglast des axialbelasteten Kreiszylinders. PhD thesis, University of Stuttgart, 1982.
12. Knoedel, P., Stabilitätsuntersuchungen an kreiszylindrischen stählernen Siloschüssen. PhD thesis, University of Karlsruhe, 1994.